The measurement of muon $g - 2$ at Fermilab

P. Girotti(*)

INFN, Sezione di Pisa - Pisa, Italy

Summary. — The Muon $g - 2$ Experiment at Fermilab (E989) was built to repeat and improve the previous E821 Experiment at Brookhaven National Laboratory (BNL), aiming to reduce the experimental error by a factor of 4 to the final accuracy of 140 parts per billion (ppb). On April 7th, 2021, the E989 collaboration published the first result based on the first year of data taking (Run-1), measuring $a_\mu = 0.001\,165\,920\,40(54)$ with a precision of 460 ppb. The measured value is consistent with the BNL measurement and strengthens the long-standing tension with the data-driven SM prediction to a combined discrepancy of 4.2σ. On the theory side, however, new efforts involving lattice-QCD techniques are starting to question the current consensus on the theoretical prediction, demanding new improvements on both the experimental and theoretical sides. The Muon $g-2$ Experiment at Fermilab has now concluded its sixth and final year of data taking, and a new result based on the Run-2 and Run-3 data was published in August 2023. This paper briefly describes the Muon $g - 2$ Experiment at Fermilab and its current status.

1. – Introduction

The muon g factor is a dimensionless quantity that relates the muon magnetic moment to the muon spin:

$$\vec{\mu} = g\frac{q}{2m}\vec{S} \ .$$
(1)

While Dirac's equation predicts that $g = 2$, quantum loop corrections to the interaction vertex between the muon and an external magnetic field effectively modify the value such that $g > 2$. The relative deviation from 2 is named the muon anomaly and is:

$$a_\mu \equiv \frac{g - 2}{2} = 0.0011659\dots \ ,$$
(2)

(*) On behalf of the Muon $g - 2$ Collaboration.

TABLE I.: Electrodynamics (QED), electroweak (EW), hadronic vacuum polarization (HVP), and hadronic light-by-light (HLBL) contributions to a_μ as computed by the Muon $g-2$ Theory Initiative in 2020 [3].

Term	Value ($\times 10^{-11}$)
a_μ^{QED}	$116\,584\,718.931 \pm 0.104$
a_μ^{EW}	153.6 ± 1.0
a_μ^{HVP}	$6\,845 \pm 40$
a_μ^{HLBL}	92 ± 18
Total SM	$116\,591\,810 \pm 43$

with its precise value depending on all the possible virtual particles participating in the loop corrections. This is the reason why a comparison between a precise measurement of such quantity and the respective calculation based on the knowledge of particle physics is of great interest. A deviation between the experimental measurement and the theoretical prediction could reveal new physics contributions in the loop corrections. Moreover, muons are particularly important in such comparisons because Beyond Standard Model interactions with massive particles contribute with mass suppression terms, $\propto \left(\frac{m_{lepton}}{M}\right)^2$. The muon is therefore $\left(\frac{105.66}{0.511}\right)^2 \approx 43000$ times more sensitive to such terms with respect to the electron [1].

The history of the muon $g-2$ is a 70 years old story of alternating experiments and theoretical calculations with ever-increasing precision on both fronts. By the end of 2020, the two values showed an interesting tension of 3.7σ. The best experimental measurement was conducted by the Brookhaven National Laboratory with a final value of [2]:

$$(3) \qquad a_\mu^{Exp}(\text{BNL, 2006}) = 0.00116592089(63) \ [540 \text{ ppb}] \,,$$

while the theoretical value was compiled by the Muon $g-2$ Theory Initiative([1]) (TI) group of physicists which organized and averaged the various contributions from QED, EW, and QCD physics to a_μ [3]:

$$(4) \qquad a_\mu^{Th}(\text{TI, 2020}) = 0.00116591810(43) \ [368 \text{ ppb}] \,.$$

Table I lists the contributions to a_μ as computed by the TI.

In this context, the Muon $g-2$ Experiment at Fermilab (E989) was built to increase the precision of the experimental measurement by a factor of four, with the goal accuracy of 140 ppb. On April 7th, 2021, the Muon $g-2$ collaboration announced the first measurement of a_μ based on the first year of data taking, which took place in 2018. The measured value is:

$$(5) \qquad a_\mu^{Exp}(\text{FNAL, 2021}) = 0.00116592040(54) \ [460 \text{ ppb}] \,,$$

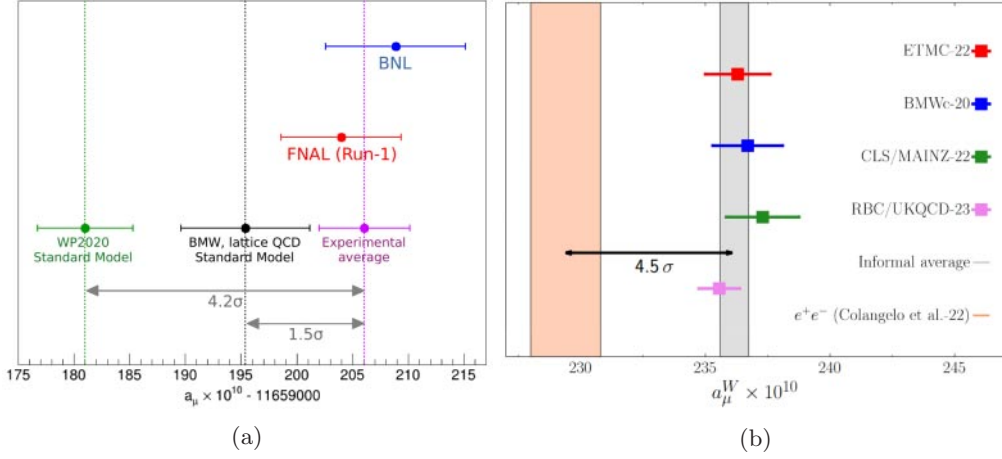
([1]) https://muon-gm2-theory.illinois.edu/

Fig. 1.: (a) Comparison between the experimental measurements of a_μ by the BNL and FNAL experiments and the two theoretical predictions based on the data-driven (WP2020) and lattice-QCD (BMW) approaches as of 2021. (b) Recent results on the hadronic vacuum polarization contribution to a_μ calculated with lattice-QCD techniques in a reduced range (window) of energies, a_μ^W, and compared to the data-driven computation (e^+e^-). Figure from [9].

which is perfectly consistent with the BNL value with a slightly improved precision of 460 ppb [4]. Combining the two results, we have the new experimental average of:

$$(6) \qquad\qquad a_\mu^{Exp}(\text{World, 2021}) = 0.00116592061(41) \ [350 \text{ ppb}] \ ,$$

and an increased discrepancy with the TI theoretical prediction of 4.2σ [4].

However, in the same period, a new theoretical calculation of the QCD contribution to a_μ based on ab-initio Lattice-QCD techniques, *i.e.*, without any external input from experimental cross-section data, was published [5]. While the hadronic light-by-light a_μ^{HLbL} term is in agreement with the data-driven estimations, the lowest-order hadronic vacuum polarization $a_\mu^{HVP,LO}$ term is creating a tension between the two methods and is moving the theoretical value of a_μ closer to the experimental one. Figure 1(a) shows the comparison between the experimental values and the two theoretical approaches. In the past few years, other groups provided preliminary results on the same quantity measured in a reduced region of energies which accounts for $\sim$30% of the total value [6-8], all in agreement with the original value. Figure 1(b) shows the comparison between the various Lattice-QCD calculations of a_μ^{HVP} in this reduced energy region. The tension that is now consolidating between the two theoretical approaches for the estimation of a_μ^{HVP} is being referred as *the new g − 2 puzzle* and remains unexplained as of today.

2. – The experiment

The Muon $g - 2$ Experiment (E989) in operation at Fermi National Accelerator Laboratory aims to measure the muon's anomalous magnetic moment with a precision of 0.14 ppm, a factor of four better than the previous BNL E821 Experiment. To achieve

Fig. 2.: Decay of the positive pion in the rest frame of reference. The spin of the muon points toward the pion as the neutrino must be left-handed because of parity violation of the weak interaction.

this precision, a statistics of $\sim$20 times the amount collected at BNL is needed, and the systematics must be contained within 100 ppb. In order to obtain a large number of observed muons, the BNL storage ring was moved from Brookhaven to Fermilab and installed in the FNAL muon campus accelerator chain, where the muon beam is cleaner and produced with a tenfold higher fill rate.

The experimental technique consists of producing a polarized and clean beam of muons, sending it to a storage ring with very uniform magnetic field, and observing the decay positrons. Three measurements are needed to calculate the muon anomaly a_μ: the muon anomalous precession frequency, the magnetic field intensity, and the beam distribution inside the storage region. The master formula is the following:

$$(7) \qquad\qquad a_\mu = \frac{\omega_a}{\tilde{\omega}_p} \frac{g_e}{2} \frac{m_\mu}{m_e} \frac{\mu_p}{\mu_e} \ ,$$

where ω_a is the muon anomalous precession frequency, and $\tilde{\omega}_p$ is the Larmor precession frequency of the proton (ω_p) convoluted with the beam distribution, representing the average field intensity experienced by the muons. The remaining factors are known with sufficient precision from other experiments. Small corrections are applied to the measured quantities of ω_a^m and $\tilde{\omega}_p^m$ due to beam dynamics effects and field transients. Further details can be found in the Run-1 accompanying papers [10,11].

2˙1. *The muon beam*. – The muons observed in the Muon $g-2$ Experiment originate from decaying pions, which are in turn produced by the collisions of an 8 GeV proton beam on a NiCrFe (*Inconel*® 600) target. After the collisions, secondary particles are focused with an electrostatic lithium lens, and pions having 3.1 GeV momentum are extracted. The pions quickly decay into muons while circulating inside a Delivery Ring, where the remaining protons get removed with a timed kick. Since pions have zero spin, the muons are emitted isotropically in the rest frame of reference, but their helicity is constrained by the weak decay, as illustrated in fig. 2. By selecting boosted muons with higher momentum, a highly polarized beam is obtained in the laboratory frame of reference. Finally, the 120-ns long muon bunches enter the Muon $g-2$ storage ring at a rate of 11.4 Hz. A superconducting inflector magnet lets the beam pass through the ring yoke into the storage region. Then, after the first quarter of an orbit, a fast pulsed kicker [12] magnet deflects the muon bunch into the final orbit, which has a radius of 7.112 m and a period of 149.2 ns. The $\sim$5000 stored muons per bunch then circulate inside the ring for 700 μs, while a set of electrostatic quadrupoles provides weak focusing for vertical confinement [13].

2˙2. *The field measurement*. – The magnet field measurement consists of various components and techniques used to determine the value of ω_p: 378 Nuclear Magnetic Resonance (NMR) fixed probes are placed along the ring under and over the vacuum chamber.

The probes keep monitoring the field during the whole data taking. Every three days during data taking, trolley runs are performed in which a mobile cylinder equipped with 17 NMR probes traverses the beam storage region to make 9000 measurements along the ring [10]. The trolley measurements produce a three-dimensional (3D) map of the magnetic field inside the storage region. The 3D map is then interpolated over the time between two consecutive trolley runs with the fixed probes data. While the magnetic field is ppm-level uniform along the beam cross section, it is necessary to know the muon distribution inside the storage ring in order to achieve an uncertainty of 70 ppb on $\tilde{\omega}_p$. For this, a set of two tracker stations observe positron tracks and extrapolate the decay vertex in the storage orbit. The beam distribution is extrapolated over the rest of the ring with data from the calorimeters and multiple dedicated simulations [11].

$\mathbf{2}^{\cdot}3$. *Muon precession frequency measurement*. – A charged particle with mass m placed in an uniform external magnetic field will follow a circular path because of the the Lorentz force, and this motion is called cyclotron motion. If the particle has spin, the spin direction will also rotate (precess) around the direction of the magnetic field. In the absence of electrical fields, and with the particle velocity and spin perpendicular to the magnetic field, the difference between the spin precession and cyclotron frequencies is the so-called anomalous precession frequency ω_a:

$$(8) \qquad \vec{\omega}_a \equiv \vec{\omega}_s - \vec{\omega}_c \simeq -\left(\frac{g-2}{2}\right)\frac{e\vec{B}}{m} \equiv -a_\mu \frac{e\vec{B}}{m} \ .$$

However, in a real experiment the particle beam is not always perfectly parallel to the storage plane, but oscillates and breathes vertically and horizontally. The anomalous precession frequency is sensible to such effects:

$$(9) \qquad \vec{\omega}_a = -\frac{e}{m}\left[a_\mu \vec{B} - \left(a_\mu - \frac{1}{\gamma^2-1}\right)\frac{\vec{\beta}\times\vec{E}}{c} - a_\mu\left(\frac{\gamma}{\gamma+1}\right)(\vec{\beta}\cdot\vec{B})\,\vec{\beta}\right] \ .$$

The storage region houses several electrostatic quadrupoles for a weak vertical focusing of the beam. This would affect the muon precession frequency, but, for a muon beam with *magic* momentum $p_\mu = 3.094$ GeV/c, corresponding to a value of $\gamma = 29.3$, the second term of eq. (9) cancels out. The remaining effect and the third term are measured separately and applied as *E-field* and *Pitch* corrections to ω_a.

The measurement principle relies on the parity-violating nature of the weak decay. The positive muons decay into a positron and two neutrinos with nearly 100% probability. In the rest frame of the muon, the highest energy decay positrons come from decays in which the neutrinos are emitted collaterally, as depicted in fig. 3. In this scenario, half of the initial rest mass of the muon is carried away by the decay positron ($E_{max} \approx 53$ MeV), while the rest is shared by the two neutrinos. Since the neutrino and anti-neutrino are traveling in the same direction, and the weak decay dictates they must have opposite helicities, their spins must be opposite. With the neutrinos' spins canceling, conservation of angular momentum forces the decay positron to carry the spin of the parent muon. The $V-A$ nature of the weak decay prefers to couple to a right-handed positron, so the high-energy decay positron depicted in fig. 3 tends to be emitted in the direction of the muon spin. Therefore, in the rest frame of the muon, the spin direction of the muon can be monitored by observing the direction at which the high energy decay positrons are
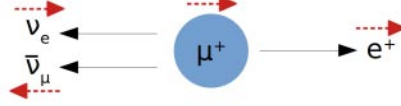
Fig. 3.: Muon decay configuration that maximizes the positron momentum and decay probability. The right-handed positron is emitted in the direction of the muon spin.

emitted. The Muon $g - 2$ Experiment is equipped with 24 electromagnetic calorimeters located around the ring with 15° azimuthal distance between each other. The asymmetry of the decay process, together with the fact that the spin precesses with respect to the momentum, results in an oscillation in the count of positrons over time. The number of detected positrons above a single energy threshold E_{th} is:

$$(10) \qquad N(t) = N_0 e^{-t/\tau}[1 + A\cos(\omega_a t + \phi)] \, ,$$

where the normalization N_0, the asymmetry A and the initial phase ϕ are all dependent on the energy threshold. τ represents the lifetime of the muon in the laboratory frame of reference, that is $\gamma\tau_\mu \simeq 64.4$ μs. Additional beam-related effects, as coherent betatron oscillations and muon losses, appear as multiplicative terms to N_0, A, and ϕ. Three different reconstruction techniques and several analysis procedures are implemented to obtain the ω_a value [14]. As an example, in the A-Weighted method the positrons counts are weighted by the asymmetry, which depends on the energy, yielding the maximum possible statistical power for a given threshold E_{th}. The typical plot showing the count of positrons over time is called *wiggle plot* and is shown in fig. 4.

The positrons are measured by 24 calorimeters, which each have a 9x6 array of PbF$_2$ crystals with size $2.5 \times 2.5 \times 14$ cm [15]. The charged particles in the electromagnetic shower generate Čerenkov photons. The choice of a pure Čerenkov material is driven by the almost instantaneous signal produced when a positron strikes, further enhanced by
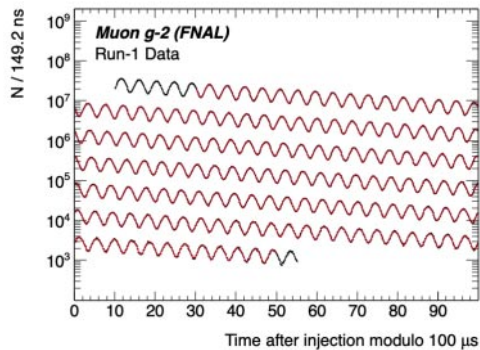

Fig. 4.: *Wiggle plot* showing the number of positrons above threshold over time. The graph is wrapped every 100 μs to show the entire measurement period. The oscillation period is $2\pi/\omega_a$ and the red curve is the fit to the data, starting at $t = 30$ μs from injection.
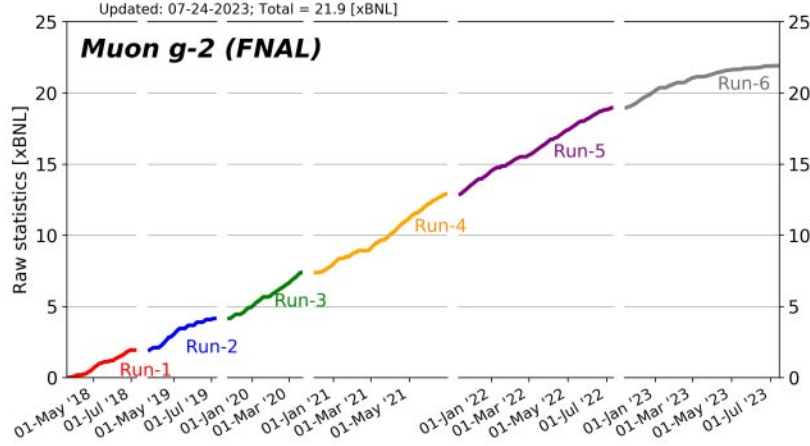
Fig. 5.: Collected statistics in the six runs of the Muon g-2 Experiment at Fermilab in terms of BNL datasets.

a black Tedlar® wrapping that absorbs part of the reflected photons. Every crystal is coupled with a Silicon PhotoMultiplier (SiPM) detector, whose signals are digitized at an 800 MHz sampling rate and chopped into 40-ns islands by on-line GPUs. A precise gain calibration of the SiPMs at the level of $\mathcal{O}(10^{-4})$ is provided by a Laser-based Calibration System [16].

3. – Current status

The Muon $g - 2$ Experiment at Fermilab just completed its sixth and final year of data taking. During the last year, it achieved and surpassed the statistical goal of 21 times the BNL experiment. Figure 5 shows the integrated number of positrons collected during the six runs.

In April 2021, the Muon $g - 2$ Collaboration released their Run-1 measurement of the muon anomaly with a precision of 460 ppb [4]. In August 2023, few months after the conference this article is about, the collaboration released their second measurement relative to the Run-2 and Run-3 data taking periods, which took place respectively in 2019 and 2020. The new value more than doubled the precision of the Run-1 result and the current FNAL value is reported here [17]:

$$(11) \qquad a_\mu^{Exp}(\text{FNAL}, 2023) = 0.00116592055(24) \times 10^{-11} \ \ [200 \text{ ppb}] \,,$$

$$(12) \qquad a_\mu^{Exp}(\text{World}, 2023) = 0.00116592059(22) \times 10^{-11} \ \ [190 \text{ ppb}] \,.$$

The new world average is now dominated by the FNAL measurement, and it currently stands at 5.1σ from the TI value of 2020. As explained in sect. **1**, however, the tensions between the theoretical approaches of the QCD contributions have to be resolved before deducing any new physics from this discrepancy.

The Muon $g - 2$ collaboration is now actively analyzing the remaining datasets, Run-4, Run-5, and Run-6, which consist of roughly 75% of the total accumulated statistics.

A new publication is expected in 2025 with a final error currently on track to beat the original goal of 140 ppb.

* * *

REFERENCES

[1] Jegerlehner F. and Nyffeler A., *Phys. Rep.*, **477** (2009) 1.
[2] Muon $g - 2$ Collaboration (Bennett G. W. *et al.*), *Phys. Rev. D*, **73** (2006) 072003.
[3] Aoyama T. *et al.*, *Phys. Rep.*, **887** (2020) 1.
[4] Muon $g - 2$ Collaboration (Abi B. *et al.*), *Phys. Rev. Lett.*, **126** (2021) 141801.
[5] Borsanyi *et al.*, *Nature*, **593** (2021) 51.
[6] Cè Marco *et al.*, *PoS*, **ICHEP2022** (414) 2023823.
[7] Cè Marco *et al.*, *Phys. Rev. D*, **106** (2022) 114502.
[8] Alexandrou C. *et al.*, *Phys. Rev. D*, **107** (2023) 074506.
[9] Sanfilippo F., talk from *NePSi23*, https://agenda.infn.it/event/32931/contributions/187824/.
[10] Muon $g - 2$ Collaboration (Albahri T. *et al.*), *Phys. Rev. A*, **103** (2021) 042208.
[11] Muon $g - 2$ Collaboration (Albahri T. *et al.*), *Phys. Rev. Accel. Beams*, **24** (2021) 044002.
[12] Schreckenberger A. P. *et al.*, *Nucl. Instrum. Methods A*, **1011** (2021) 165597.
[13] Kim On *et al.*, *New J. Phys.*, **22** (2020) 063002.
[14] Muon $g - 2$ Collaboration (Albahri T. *et al.*), *Phys. Rev. D*, **103** (2021) 072002.
[15] Alonzi L. P. *et al.*, *Nucl. Instrum. Methods Phys. Res. A*, **824** (2016) 718.
[16] Anastasi A. *et al.*, *JINST*, **14** (2019) P11025.
[17] Muon $g - 2$ Collaboration (Aguillard D. P. *et al.*), arXiv:2308.06230, to be published in *Phys. Rev. Lett.* (2023).